

Quest for rare events in mesoscopic disordered metals

Branislav K. Nikolić

Department of Physics, Georgetown University, Washington, DC 20057-0995

(Received 27 June 2001; published 29 November 2001)

The study reports on the first large statistics numerical experiment searching for rare eigenstates of anomalously high amplitudes in three-dimensional diffusive metallic conductors. Only a small fraction of a huge number of investigated eigenfunctions generates the far asymptotic tail of their amplitude distribution function. The relevance of the relationship between disorder and spectral averaging, as well as of the quantum transport properties of the investigated mesoscopic samples, for the numerical exploration of eigenstate statistics is divulged. The quest provides exact results to serve as a reference point for understanding the limits of approximations employed in different analytical predictions and, therefore, the physics (quantum vs semiclassical) behind large deviations from the universal predictions of random matrix theory.

DOI: 10.1103/PhysRevB.65.012201

PACS number(s): 73.23.-b, 72.15.Rn, 05.45.Mt, 05.40.-a

Despite years of extensive studies, initiated by the seminal work of Anderson,¹ the problem of a quantum particle in a random potential (“disorder”) still poses challenges. The biggest shift in approach and intuition came with the advent of mesoscopic quantum physics²—from critical phenomena inspired description³ of the localization-delocalization (LD) transition to the realization that a complete understanding of quantum interference effects, generating LD (zero-temperature) transition for strong enough disorder, requires studying the full distribution functions⁴ of relevant physical quantities (such as conductance, the local density of states, current relaxation times, etc.⁵) in finite-size disordered electronic systems. Even in diffusive metallic conductors, the tails of such distribution functions show large deviations from the ubiquitous Gaussian distributions, expected in the limit of infinite dimensionless zero-temperature conductance $g = G/(e^2/\pi\hbar)$. These asymptotic tails are putative precursors of the developing Anderson localization occurring at $g \sim 1$.

A conjecture about unusual eigenstates being microscopically responsible for the asymptotic tails⁴ of various distribution functions related to transport was put forward early in the development of the mesoscopic program.⁵ However, it is only recently⁶ that eigenstate statistics have come into the focus of mesoscopic community. Similar investigations in the guise of quantum chaos^{2,7} started a decade earlier (leading to the concept of scarring⁸ in quantum chaotic wave functions). Thus the notion of “prelocalized” states has emerged from the studies of quantum disordered systems^{5,9,10} of finite g . In three-dimensional (3D) conductors these states have sharp amplitude peaks on the top of a homogeneous background. Their appearance, even in good metals, has been viewed as a sign of an incipient localization.⁵ However, the nonuniversality of the prelocalized states tempers this view,¹¹ but suggests that nonsemiclassical effects¹¹ might be important for some phenomena in systems whose typical transport properties are properly described by semiclassical theories [including the perturbative quantum corrections¹² $\sim O(g^{-1})$]. Here I provide an insight into the weirdness of such states: Fig. 1 plots the amplitude spikes of an anomalously rare prelocalized state, to be contrasted with the amplitudes of an ordinary extended state shown in the same

figure. The study of prelocalized states not only reveals mathematical peculiarities of the eigenproblem of random Hamiltonians, but is relevant for various quantum transport experiments, such as e.g., tunneling experiments on quantum dots where coupling to external leads depends sensitively on the local properties of wave functions.¹³ By exploiting the correspondence between the Schrödinger and Maxwell equations in microwave cavities, it has become possible to probe directly the microscopic structure of quantum chaotic or disordered wave functions.¹⁴

This study presents a numerical result for the statistics of eigenfunction “intensities” $|\Psi_\alpha(\mathbf{r})|^2$ in closed 3D mesoscopic conductors which are diffusive ($L \gg l$) (L and l being the size of the system and elastic mean free path, respectively), metallic ($g \gg 1$), and weakly disordered ($k_F l \gg 1$) (k_F is the Fermi wave vector). The statistical properties of eigenstates are described by a disorder-averaged distribution function¹⁰

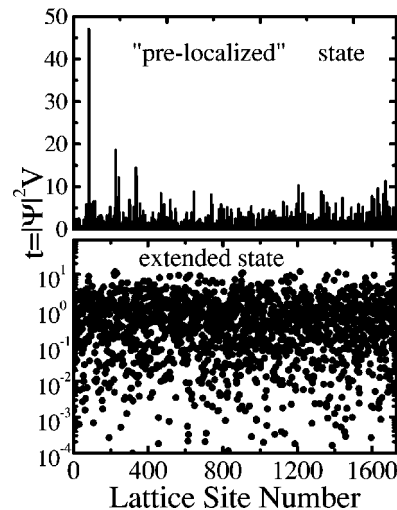


FIG. 1. Examples of eigenstates in the band center of a delocalized phase in the Anderson model with $W=5$. The average conductance at half-filling is $g \approx 12$, entailing an anomalous rarity of the “prelocalized” states. For plotting the eigenfunction values in three dimension, the sites \mathbf{m} of the 12^3 lattice are mapped onto $\{1, \dots, 1728\}$ in lexicographic order, i.e., $\mathbf{m} \equiv (m_x, m_y, m_z) \mapsto 144(m_x - 1) + 12(m_y - 1) + m_z$.

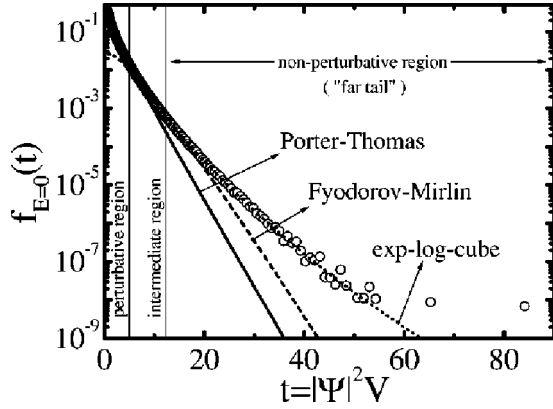


FIG. 2. Statistics of eigenfunctions in the band center of the Anderson model with diagonal disorder $W=5$ on a simple cubic lattice 12^3 . The numerically calculated distribution $f_{E=0}(t)$ is fitted with the leading order of the Fyodorov-Mirlin correction, $f_{\text{FM}}(t)[1 + 0.04(3/2 - 3t + t^2/2)]$, to PT distribution (valid in the perturbative region); and exp-log-cube, $0.0256 \exp(-0.239 \ln^3 t)$, at large deviations from $f_{\text{PT}}(t)$ in the nonperturbative region. A similar fit is achieved with exp-log-cube, $0.045 \exp[-0.19 \ln^3(t/0.72)]$, akin to $f_{\text{NLSM}}(t)$.

$$f_E(t) = \frac{1}{\rho(E)N} \left\langle \sum_{\mathbf{r}, \alpha} \delta(t - |\Psi_\alpha(\mathbf{r})|^2 V) \delta(E - E_\alpha) \right\rangle \quad (1)$$

on N discrete points \mathbf{r} inside a sample of volume V . Here $\rho(E) = \langle \sum_\alpha \delta(E - E_\alpha) \rangle$ is the mean level density at energy E , and $\langle \dots \rangle$ denotes disorder averaging. Finite-size disordered samples are modeled by a tight-binding Hamiltonian

$$\hat{H} = \sum_{\mathbf{m}} \varepsilon_{\mathbf{m}} |\mathbf{m}\rangle \langle \mathbf{m}| + \sum_{\langle \mathbf{m}, \mathbf{n} \rangle} t_{\mathbf{m}\mathbf{n}} |\mathbf{m}\rangle \langle \mathbf{n}|, \quad (2)$$

with nearest-neighbor hopping $t_{\mathbf{m}\mathbf{n}} = 1$ (unit of energy) between s orbitals $\langle \mathbf{r} | \mathbf{m} \rangle = \psi(\mathbf{r} - \mathbf{m})$ located on sites \mathbf{m} of a simple cubic lattice of size $L = 12a$ (a being the lattice spacing). Periodic boundary conditions are chosen in all directions. The disorder is simulated by taking the potential energy $\varepsilon_{\mathbf{m}}$ to be a uniformly distributed random variable over the interval $[-W/2, W/2]$. This is a standard Anderson model of localization,¹ where weak disorder is introduced by $W=5$ (the model can also be viewed as a discretized version of the problem of a single particle in a continuous random potential).

The eigenproblem of Eq. (2) is solved exactly by numerical diagonalization. A small energy window $\Delta E = 0.007$ is positioned around $E=0$, picking up 0–3 states in each of the 30000 conductors with different impurity configurations. This large ensemble makes it possible to obtain a well-defined far tail (Fig. 2), stemming from the amplitudes of prelocalized states (the far tail has been investigated previously by numerical simulation only in low-dimensional systems^{15,16} where, strictly speaking, all states are localized even for weak disorder,³ albeit with an exponential localization length in two dimensions).

In both generic quantum chaotic and quantum-disordered systems eigenstates are characterized solely by their energy (the only constant of motion) instead of a set of quantum

numbers. Their classical counterparts are nonintegrable—in the entire phase space for “hard” chaos.⁷ Quantum chaos implies a semiclassical approximation⁷ ($\hbar \rightarrow 0$), and is less efficient^{14,16} in localizing chaotic wave functions through scars than localization by quantum disorder,¹⁷ due to interference effects in the diffusive motion. Since eigenstates and eigenvalues cannot be obtained analytically, one usually resorts to some statistical treatment. The unifying concepts in this pursuit come from approaches like random matrix theory⁷ (RMT) and its justification (note that matrix elements of Hamiltonians of disordered solids are spatially dependent, and therefore do not satisfy standard assumptions of RMT) through the supersymmetric nonlinear σ -model¹² (NLSM). RMT gives universal predictions for the level and eigenstate statistics, which are applicable in the limit $g \rightarrow \infty$. Its answer for $f_E(t)$, in time-reversal invariant systems, is given by the Porter-Thomas⁷ (PT) distribution function

$$f_{\text{PT}}(t) = \frac{1}{\sqrt{2\pi t}} \exp(-t/2). \quad (3)$$

Within RMT, $\Psi_\alpha(\mathbf{r})$ is a Gaussian random variable, thereby leading to χ^2 distribution of intensities. The NLSM allows one to study the finite g corrections to the universal properties of weakly disordered ($k_F l \gg 1$) samples, which turn out to be determined by the properties of classical diffusion.⁶ The distribution function $f_{E=0}(t)$ is contrasted with $f_{\text{PT}}(t)$ in Fig. 2. For $t \gtrsim 5$, a deviation in the tail starts to develop, eventually becoming a few orders of magnitude greater probability than the RMT prediction for the appearance of states with high-amplitude splashes. However, the disorder is so weak that the large- t limit tail is shorter, and composed of smaller values of $f_E(t)$ than some quantum chaotic tails attributed to scarring.^{8,16} Small deviations from PT distribution are taken into account through a perturbative (weak-localization) correction¹⁸

$$f_{\text{FM}}(t) = f_{\text{PT}}(t) \left[1 + \frac{\kappa}{2} \left(\frac{3}{2} - 3t + \frac{t^2}{2} \right) + O(g^{-2}) \right], \quad (4)$$

derived by Fyodorov and Mirlin (FM)¹⁸ for $t \ll \kappa^{-1/2}$. Here κ ($\sim L/g l$ in three dimensions) has the meaning of a classical (time-integrated) return probability for a diffusive particle.⁶

In a region of considerable deviations, where $f_E(t)$ decays much slower than $f_{\text{PT}}(t)$, one has to use nonperturbative predictions for the asymptotics of $f_E(t)$ in mesoscopic metals.¹² They employ either NLSM techniques,⁶

$$f_{\text{NLSM}}(t) \sim \exp\left[-\frac{1}{4\kappa} \ln^3(\kappa t)\right], \quad t \gtrsim \kappa^{-1}, \quad (5)$$

or the “direct optimal fluctuation (DOF) method” of Ref. 11 (where only the leading term of exp-log-cube asymptotics is evaluated explicitly¹¹)

$$f_{\text{DOF}}(t) \sim \exp[-C_{\text{DOF}} k_F l \ln^3 t], \quad (6)$$

aiming to describe the short-scale (and non-semiclassical) structure of the solutions of Schrödinger equation in a white-

noise disorder. The intermediate region of amplitudes (Fig. 2) is covered in the NLSM formalism by

$$f(t) \approx \frac{1}{\sqrt{2\pi t}} \exp\left[\frac{1}{2}\left(-t + \frac{\kappa t^2}{2} + \dots\right)\right], \quad \frac{1}{\sqrt{\kappa}} \lesssim t \lesssim \frac{1}{\kappa}, \quad (7)$$

where a correction in the exponent is large compared to unity, but small compared to the leading RMT term.¹⁰

Numerical techniques provide the means to solve exactly the (discretized) Schrödinger equation for a quantum particle in an arbitrary strong random potential, i.e., for all transport regimes—from semiclassical to strongly localized.¹⁹ Such solutions are a good reference point from which one can gauge analytical predictions and their “neglect” of those effects which are hard to deal with within a specific formalism. Analogous numerical investigations of $f_E(t)$ in quantum chaotic systems have typically dealt with a single set of eigenstates,¹⁶ since an impurity ensemble is absent in standard clean examples of quantum chaos (such as, e.g., quantum billiards¹⁴). Even in quantum-disordered systems, the computation of $f_E(t)$ involved only relatively small ensembles of disordered conductors, or combined disorder and spectral averages (the disorder averaging is supposed to improve the statistics, while claiming that individual eigenstate would show more or less the same behavior¹⁶). Thus the natural questions arise: Is an enormous ensemble of disordered conductors indispensable to obtain complete $f_E(t)$ in a good metal? Can spectral averaging [i.e., a wide broadening of $\delta(E - E_\alpha)$ in Eq. (1) into a box function of the width ΔE] be used to facilitate this quest? Both questions demand empirical answers, which are readily obtained from Fig. 3. Only a small fraction of all investigated eigenfunctions exhibits the highest observed amplitudes [panel (a) in Fig. 3]. Therefore, one has to search for special configurations of disorder where quantum interference effects can lead to large wavefunction inhomogeneities. These are anomalously rare in weakly disordered conductors, i.e., the tail of $f_E(t)$ is not generated by a large number of more or less equal-weight impurity configurations.¹¹ The effect of spectral averaging is not *a priori* obvious.²⁰ That is, the short-scale physics to be discussed below can correlate eigenstates with neighboring eigenvalues, and therefore produce artifacts of the numerical procedure employed to obtain $f_E(t)$ in a finite-size system with a discrete spectrum, when the original definition [Eq. (1)] in terms of δ functions is abandoned. Nonetheless, the comparison of $f_E(t)$ from Fig. 2 and the one obtained from the same impurity ensemble but with $\Delta E = 0.3$ (where 62 states are collected, on average, from each sample) suggests that combined impurity ensemble and reasonable spectral averaging might be the most efficient way to obtain a long and smooth far tail (Fig. 3).

Mesoscopic transport properties of finite-size samples can be fully delineated from the “measurement” on a computer. This offers a simple way of comparing the above formulas to the observation in real systems—instead of trying to deduce the functional form of $f_E(t)$ phenomenologically (which is usually inconclusive because of the possibility to fit different functions reasonably well), one can use the “measured” val-

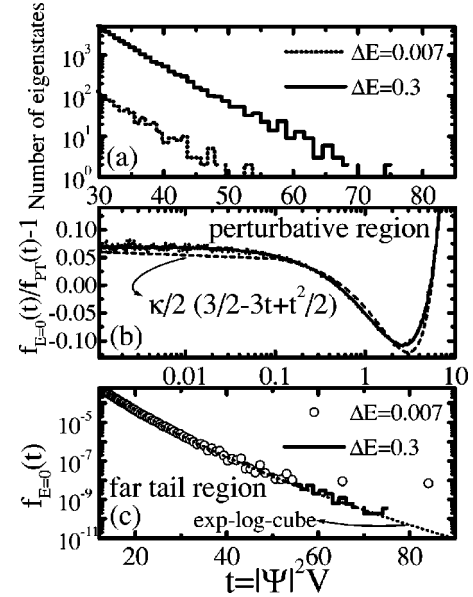


FIG. 3. Comparison of the disorder average (over the impurity ensemble) and combined disorder and spectral averaging [over a small interval ΔE used to broaden $\delta(E - E_\alpha)$ from Eq. (1) into a box function] in computing $f_E(t)$: (a) Histogram of the number of eigenstates which exhibit the largest amplitude splashes determining the very end of the far tail of the distribution of $|\Psi_\alpha(\mathbf{r})|^2$. Both histograms are defined by only 1.4% of 43342 or 1.86×10^6 eigenstates collected in the interval $\Delta E = 0.007$ or $\Delta E = 0.3$ around $E = 0$, respectively. (b) Perturbative region and FM fit (note a small discrepancy between the data and the fit, which increase upon approaching the upper boundary $W \approx 6$ of the semiclassical transport regime). (c) Far tail region and exp-log-cube fit.

ues, adjust the free parameters, and, if the analytical expressions work, explore the viability of physics behind the raw numbers. The quantitative understanding of transport is also a prerequisite for another reason. The lattice size sets a lower limit on the disorder strength, which ensures the diffusive transport regime ($L \gg l$). When disorder is too strong, semiclassical parameters become nonsensical ($l < a$), although the conductor might still be far away ($g \gg 1$) from the LD transition point.^{3,21} On the other hand, only for strong enough disorder is the far tail reasonably long (Fig. 2) enough to allow the extraction of reliable fitting parameters. The interplay of these three limits leaves a narrow range $4 \lesssim W \lesssim 6$ of possible disorder strengths in this study.

The exact zero-temperature disorder-averaged conductance is calculated from the two-probe Landauer formula $g(E_F) = \text{Tr}[\mathbf{t}(E_F)\mathbf{t}^\dagger(E_F)] \approx 12$ (at $E_F = 0$).²¹ The Fermi wave vector $k_F \approx 2.8/a$, averaged over the Fermi surface $E_F = 0$ of a simple cubic lattice, serves as a counterpart of k_F used in theoretical simplifications which assume a Fermi sphere. For $W = 5$, g is dominated by the semiclassical effects.²¹ Thus I use the Bloch-Boltzmann formalism (applicable when $k_F l \gg 1$), in the Born approximation for the scattering on a single impurity, to obtain²¹ $l \approx 1.4a$ ($k_F l \approx 4$).

Small deviations (both in the body and in the tail) of the numerical $f_{E=0}(t)$ from the PT distribution are well explained by $f_{FM}(t)$ [panel (b) in Fig. 3]. However, $\kappa \approx 0.08$

extracted from the fit is much larger than the diffusive and universal¹⁸ (i.e., independent of the details of disorder) $\kappa_{\text{diff}} = (2/g\pi^2)\sum_{\mathbf{q}}\exp(-\mathcal{D}\mathbf{q}^2\tau)/\mathbf{q}^2L^2 = 0.018$. The exact value of the sum over the diffusion modes [$\mathbf{q} = (2\pi n_x/L, 2\pi n_y/L, 2\pi n_z/L)$], being quantized by the periodic boundary conditions $n_x, n_y, n_z = \pm 1, \pm 2, \dots$], is evaluated numerically, where an exponential cutoff provides the necessary ultraviolet regularization at $|\mathbf{q}| \sim l^{-1}$ ($\mathcal{D} = v_F^2\tau/3$ is a classical diffusion constant). The divergence of the sum in three dimensions necessitates going beyond the diffusion approximation of the NLSM, implying that short-range spatial correlations become important. This is to be contrasted with the long-range correlations (described by the soft modes of the NLSM) in low-dimensional systems where κ_{diff} is a convergent parameter-free number. Therefore, to reproduce the fitted κ , the other relevant (“ballistic” and nonuniversal) contribution $\kappa_{\text{ball}} \sim (k_F l)^{-1}$, arising from quantum dynamics on time scales shorter than the elastic mean free time^{6,22} τ , has to be included; $\kappa = \kappa_{\text{diff}} + \kappa_{\text{ball}} \sim (k_F l)^{-2} + (k_F l)^{-1}$. The intermediate region is poorly described by formula (7).

The beginning of the far tail $t \gtrsim \kappa^{-1} \approx 12$ is located approximately using the fitted κ from the perturbative region. The exp-log-cube formulas [Eqs. (5) and (6)] imply that this region should be explained by an exponential function of a cubic polynomial $C_p \exp(-C_3 \ln^3 t - C_2 \ln^2 t - C_1 \ln t)$. The fit, however, cannot give the accurate values for all four parameters simultaneously. On the other hand, a fit including just the cubic term $C_p \exp(-C_3 \ln^3 t)$ works well (Figs. 2 and 3), giving $C_3 = 0.239$ and $C_p = 0.0256$. The NLSM universal result goes beyond predicting only the prefactor of the leading log-cube term by including the lower powers of $\ln t$. This form also fits the data reasonably well with $\kappa = 1.39$ and the log-cube prefactor $C_{\text{NLSM}} \approx 0.19$ [which is close to the prefactor $1/4\kappa = 0.18$ in $f_{\text{NLSM}}(t)$]. Nevertheless, there are two major puzzles with $f_{\text{NLSM}}(t)$ fitting the numerical data: (1)

Inasmuch as κ is a characteristic quantity of classical diffusive dynamics, determining both perturbative and nonperturbative corrections (within the framework of NLSM) to the RMT picture,⁶ the different values, required here for different intervals of amplitudes in Fig. 2, are hard to reconcile (regardless of the dynamical origin of κ). (2) Since $\kappa_{\text{diff}} \sim (k_F l)^{-2}$, the log-cube prefactor has the form $1/4\kappa \sim (k_F l)^2$. However, the investigation of different ensembles for a range of l ($\propto W^{-2}$) hints at the prefactor (C_3 or C_{NLSM}) being close to a linear function of $k_F l$ as is the case with²³ $f_{\text{DOF}}(t)$ (an unexpected sublinear prefactor behavior is also seen in the 2D Anderson model).

Thus the exp-log-cube formulas *could* account for the far tail of the statistics of eigenstates in the Anderson model. However, their expected parameters are inadequate, suggesting that short-scale effects below l , which are to be treated by the extension of semiclassical methods to subdiffusive dynamics²² and/or fully quantum theory,¹¹ are essential (even for small deviations from RMT statistics). They lead to strong dependence of eigenstate statistics in three dimensions on microscopic details of a random potential.⁶ It remains to be seen if the log-cube prefactor can be explained by examining the short-scale physics (thereby going beyond standard diffusive NLSM corrections, which are semiclassical in nature and universal). The Anderson model can hardly satisfy some key assumptions of the “direct optimal fluctuation method,”¹¹ while the ballistic NLSM,⁹ as yet, has only reproduced the diffusive NLSM result.¹¹

I am grateful to I. E. Smolyarenko for initiation into this problem and A. D. Mirlin for important clarifications. Essential help along the quest was provided by V. Z. Cerovski. Financial support from ONR Grant No. N00014-99-1-0328 is acknowledged.

¹P.W. Anderson, Phys. Rev. **109**, 1492 (1958).

²*Mesoscopic Quantum Physics*, edited by E. Akkermans, J.-L. Pichard, and J. Zinn-Justin, Les Houches Session LXI, 1994 (North-Holland, Amsterdam, 1995).

³E. Abrahams *et al.*, Phys. Rev. Lett. **42**, 673 (1979).

⁴M. Janssen, Phys. Rep. **295**, 1 (1998).

⁵B. L. Altshuler, V. E. Kravtsov, and I. V. Lerner, in *Mesoscopic Phenomena in Solids*, edited by B. L. Altshuler, P. A. Lee, and R. A. Webb (North-Holland, Amsterdam, 1991).

⁶A. D. Mirlin, Phys. Rep. **326**, 259 (2000).

⁷T. Ghur, A. Müller-Groeling, and H. A. Widenmüller, Phys. Rep. **299**, 189 (1998).

⁸E. J. Heller, Phys. Rev. Lett. **53**, 1515 (1984); L. Kaplan, *ibid.* **80**, 2582 (1998).

⁹B. A. Muzykantskii and D. E. Khmelnitskii, Phys. Rev. B **51**, 5480 (1995).

¹⁰V. I. Fal’ko and K. B. Efetov, Phys. Rev. B **52**, 17 413 (1995).

¹¹I. E. Smolyarenko and B. L. Altshuler, Phys. Rev. B **55**, 10 451 (1997).

¹²K. B. Efetov, *Supersymmetry in Disorder and Chaos* (Cambridge University Press, Cambridge, 1997).

¹³J. A. Folk *et al.*, Phys. Rev. Lett. **76**, 1699 (1996); A. M. Chang *et al.*, *ibid.* **76**, 1695 (1996).

¹⁴P. Pradhan and S. Sridhar, Phys. Rev. Lett. **85**, 2360 (2000).

¹⁵V. Uski *et al.*, Phys. Rev. B **62**, R7699 (2000).

¹⁶K. Müller *et al.*, Phys. Rev. Lett. **78**, 215 (1997).

¹⁷A border between “quantum chaos” and “quantum disorder” for a particle in a random potential was drawn in I. L. Aleiner and A. I. Larkin, Phys. Rev. B **54**, 14 423 (1996).

¹⁸Y. V. Fyodorov and A. D. Mirlin, Phys. Rev. B **51**, 13 403 (1995).

¹⁹B. K. Nikolić, Phys. Rev. B **64**, 014203 (2001).

²⁰R. E. Prange, Phys. Rev. Lett. **78**, 2280 (1997).

²¹B. K. Nikolić and P. B. Allen, Phys. Rev. B **63**, 020201(R) (2001).

²²Ya. M. Blanter, A. D. Mirlin, and B. A. Muzykantskii, Phys. Rev. B **63**, 235315 (2001).

²³B. K. Nikolić and V. Z. Cerovski cond-mat/0110639 (unpublished).